ELSEVIER

Carbohydrate Polymers 52 (2003) 67–85

Carbohydrate Polymers

www.elsevier.com/locate/carbpol

Rheological properties of inulin–waxy maize starch systems

J.E. Zimeri, J.L. Kokini*

center for Advanced Food Technology, Department of Food Science, Cook College, Rutgers University, 65 Dudley Road, New Brunswick, NJ 08901-8529, USA

Received 1 July 2002; revised 12 September 2002; accepted 13 September 2002

Abstract

The rheological properties of mixed systems of inulin and waxy maize starch (WMS) were studied, as a model of carbohydrate–carbohydrate interactions in foods. Steady shear and oscillatory rheological properties were analyzed using a strain-controlled rheometer. Steady shear data were satisfactorily fitted to the Carreau model. The data were also fitted to the Herschel–Bulkley model. Concentrated inulin gels presented static and dynamic yield stresses. Phase inversion from a WMS-continuous system to an inulin-continuous system, manifested as a sudden change in rheological properties, was observed in samples with a total polymer concentration ≥30% (w/w, w.b.). In order to validate the oscillatory rheological data, some samples were subjected to stress relaxation experiments and both types of data were compared, showing a satisfactory agreement. The Cox–Merz rule, which relates steady shear and dynamic material functions, was not followed by most of the samples. An extended Cox–Merz rule was applied to the analysis of concentrated inulin gels.

Keywords: Inulin; Waxy maize starch; Cox–Merz rule; Yield stress; Stress relaxation

1. Introduction

Inulin, a fructooligosaccharide, is used either as a macronutrient substitute or as a supplement added in foods mainly for its nutritional properties. It combines with water to produce the same texture and mouthfeel as fat in water-based foods such as dairy products and table spreads, as well as baked goods, fillings, frozen desserts and dressings (Niness, 1999; Schaller-Povolny & Smith, 1999). Inulin consists of fructose molecules linked by β(2–1) glycosidic bonds, which are responsible for its nutritional characteristics. It may contain either a terminal β-D-fructose or an α-D-glucose molecule (Roberfroid, Gibson, & Delzenne, 1993). Standard inulin has a degree of polymerization of 2–60; high performance (HP) forms of inulin have an average degree of polymerization of 25 (Roberfroid, 1999b).

Although inulin's nutritional properties have been thoroughly studied (Roberfroid et al., 1993; Roberfroid, 1999a,b, 2000), its physicochemical properties and interactions with other food biopolymers have just begun to be characterized. Zimeri and Kokini (2002) investigated the effect of moisture content on inulin's crystallinity and glass transition temperature (T_g) at low moisture contents (<20% w.b.). Native inulin was found to be a semi-crystalline material, which, at 25 °C and storage water activity values (a_w) <0.75, was present in the glassy state. When pre-solubilized, dried and stored at low moisture contents, inulin's relative crystallinity was low (~13%); when stored at conditions above T_g ($a_w > 0.75$), it recrystallized and reached native inulin's crystallinity level (~42%) (Zimeri & Kokini, 2002). On the investigation of the effect of inulin on the physicochemical characteristics of waxy maize starch (WMS) in limited moisture environments, Zimeri and Kokini (2003) determined that concentrated mixed samples presented two individual T_g's, which corresponded to those of the individual components, evidence of a lack of interaction between them. Thus, it was concluded that phase separation had occurred.

When examining the structure-function of biopolymer systems at high moisture contents, rheological properties play a main role. According to Martinez and Williams (1980), the viscous properties of a binary biopolymer blend can be written as $\eta(\eta_A, \eta_B, S)$ and $\eta^*(\eta_A^*, \eta_B^*, S)$, where η = apparent viscosity, η^* = complex viscosity, A and B represent the pure components and S represents a generalized structure parameter, which itself is a function of

* Corresponding author. Tel.: +1-732-932-8306; fax: +1-732-932-8690.
E-mail address: kokini@aesop.rutgers.edu (J.L. Kokini).

0144-8617/03/$ - see front matter © 2002 Elsevier Science Ltd. All rights reserved.
PII: S0144-8617(02)00268-0

volume fraction (ϕ), η_A, η_B, surface tension and the history of sample preparation. Utracki (1991) grouped all polymers according to their viscosity–concentration dependence in relation to the log–additivity rule: $\log\eta = \sum_i \phi_i \log\eta_i$, in which ϕ_i and η_i represent volume fraction and zero-shear viscosity (η_0) of the ith component in the blend, respectively. Utracki (1991) also indicated that excepting general purpose mixing rules, as the one just presented, there is no equation allowing the systematic prediction of the concentration dependence of immiscible blend viscosity.

The viscosity of dense suspensions is strongly influenced by particle arrangement at high volume fractions and flow (Gray & Bonnecaze, 1998). Most suspensions flow only when their structure, which may consist in a network that prevents flow, has been degraded by a large enough applied stress, referred to as yield stress (Zhu, Sun, Papadopoulos, & De Kee, 2001). Yield stress is a material property that occurs at the transition between solid-like and liquid-like behavior. Materials that exhibit yield stress include colloidal suspensions (<1 μm), in which particle–particle interactions are relevant (Husband, Aksel, & Gleissle, 1993). In addition to interacting particles suspended in low viscosity liquids, highly filled polymer melts of moderate elasticity but high viscosity, and filled or unfilled polymer melts of high viscoelasticity may also exhibit yield stresses (Doraiswamy et al., 1991). According to Bonnecaze and Brady (1992), in the shear stress vs. shear rate profile of a material having yield stress, the stress increases at first almost linearly (stress proportional to strain), confirming the elastic nature of the material before the yield point. The slope of the curve begins to decrease at the limit of reversibility for the material (elastic-limit yield stress), at which plastic or non-linear elastic behavior is observed, until it reaches a maxima (static yield stress, which corresponds to the minimum stress necessary for the unbounded strain or deformation of the material), after which the material response changes from solid to liquid-like (the suspension flows). The plateau stress for large strains is referred to as the dynamic yield stress, which is equivalent to the extrapolated stress to zero-shear rate in the plot of stress vs. shear rate (Bonnecaze & Brady, 1992; Zhu et al., 2001), as well as the yield stress which appears as a material parameter in constitutive models (Husband et al., 1993).

Phase behavior in mixed biopolymer systems has also been assessed via rheological measurements. For example, the phase behavior and rheology of mixed polymer systems containing starch was studied by Annable, Fitton, Harris, Phillips, and Williams (1994). With increasing gum arabic concentration ($>15\%$), the storage modulus (G') was found to decrease and polymer segregation occurred leading to a two-phase system. In 1993, Kasapis et al. studied the phase separation in mixed gels of gelatin–maltodextrin systems. The occurrence of phase inversion was determined by detecting a discontinuity on the plot of gel-time vs. concentration. Manoj, Kasapis, and Chronakis (1996) determined that maltodextrin–caseinate systems resulted in a composite system whose phase inversion from a maltodextrin-continuous network with discontinuous protein inclusions to a caseinate dispersion suspending the maltodextrin particles was determined by the weight ratio of the two components in the blend, and affected the rheological properties of the system. On the other hand, Abdulmola, Hember, Richardson, and Morris (1996) determined that the addition of starch to solutions of xanthan caused an increase in moduli, and that the addition of xanthan promoted association between the gelatinized starch granules. Mohammed, Hember, Richardson, and Morris (1998) studied the co-gelation of agarose and WMS, observing a phase inversion from the change in the moduli. Astruc and Navard (2000) suggested that for two-phase immiscible polymer blends, shear rate and elasticity of the two phases constitute additional parameters that determine final morphology. Thus, the more elastic phase will tend to encapsulate the less elastic one and form the matrix.

The objective of the present study is to characterize the effects of concentration on the rheological properties of a mixed biopolymer system of inulin and WMS in high moisture environments, as a model of carbohydrate–carbohydrate interactions in foods. The rheological properties will be linked to morphology and phase behavior in a future publication.

2. Materials and methods

2.1. Sample preparation

Inulin (Raftiline® HP, $>99.5\%$ pure, donated by Orafti, Malvern, PA), waxy maize starch (WMS, 98% amylopectin, obtained as Amioca™ from National Starch, Bridgewater, NJ) and mixtures were prepared in the following total polymer concentrations (w/w, w.b.): 2, 5, 10, 20, 30 and 40%, at ratios of inulin to WMS of 0:10, 25:75, 50:50, 75:25 and 10:0. Powders were mixed and dispersed in deionized water in a Helmco–Lacy waterproof hot cup (Star Mfg. Co., St Loius, MO). The cup was connected to a variable autotransformer (Powerstat, The Superior Electric Co., Bristol, CT), which allowed for heating rate regulation; thus, a high heating rate minimized moisture loss while preparing the samples. Temperature was measured with a thermometer. Mixing was provided via a propeller, attached to a mixer (Model LR-41A, Yamato, Japan), operated at a speed of 350 rpm. Samples were then mixed using a stir plate at 90°C for 30 min., to ensure that thorough mixing was achieved. Alluminium foil was used to cover the samples in order to prevent moisture evaporation. Samples were cooled down at room temperature and stored for 24 h previous to analysis to avoid the presence of bubbles formed during heating and mixing.

2.2. Rheological analysis

Small deformation oscillatory experiments were conducted using a strain-controlled rheometer (Advanced Rheometric Expansion System (ARES), Rheometrics, Piscataway, NJ). Couette (32 mm o.d. bob, 34 mm i.d. cup) and parallel plate (25 and 50 mm diameter) geometries were used, depending on the samples' viscosity. Cone and plate geometry (interplaten gap = 0.05 mm) was not used due to possible occlusion by the inulin phase (inulin gels presented a highly aggregated structure). Steady shear experiments (η vs. $\dot{\gamma}$) were conducted at increasing $\dot{\gamma}$ values ranging between 10^{-2} and 10^{3} s^{-1}, at a frequency (ω) of 1 Hz (6.28 rad/s). In order to avoid underestimation of viscosity and yield stress due to slip (particle depletion near the wall), the surface of the plates was roughened by attaching sand paper (No. 60, aluminum oxide, 3 M) using double sided scotch tape, following the method suggested by Zhu et al. (2001). Another advantage of using this methodology is that viscosity dependence on gap width is eliminated (Zhu et al., 2001).

Dynamic oscillatory rheological measurements (η^* vs. ω) were conducted at ω values ranging between 10^{-1} and 10^{3} rad/sec, which generated ω-dependent profiles of the storage modulus (G'), loss modulus (G''), and tangent δ ($\tan\delta$). A new sample was used in every measurement to avoid structure modification by rheological measurements. The used strain corresponded to the maximum found within the linear viscoelastic region of the material under study. In order to avoid dehydration during measurements, the samples were thinly coated with mineral oil. Four replicate measurements were conducted as a minimum and reported data correspond to the average of these measurements.

Stress relaxation tests were conducted using the same tool geometrics described above. The imposed strain amplitude was chosen so that its value fell within the linear viscoelastic response of the materials under study. The experiments resulted in a plot of the relaxation modulus, $G(t)$, vs. time. G(t) was also calculated from the dynamic oscillatory data, transformation performed by the ARES Orchestrator software (Rheometrics, Piscataway, NJ). Data from both origins were compared.

3. Results and discussion

3.1. Behavior vs. concentration

According to Carriere (1998), the transition from dilute to semi-dilute solution behavior in polymers is designated as c^*. At concentrations higher than c^*, the polymer chains become highly entangled and conformational dynamics are governed by chain–chain interactions. The transition from the semi-dilute to concentrated solution behavior is designated as c^{**}. Carriere (1998) determined that for WMS, the c^* value corresponded to 0.014 g/ml and the c^{**} corresponded to 0.048 g/ml. According to these values, the samples under study presented dilute solution behavior at starch concentrations of 2% 75:25 (inulin to WMS ratio) and below, semi-dilute solution behavior at concentrations between 2% 50:50 and 2% 0:10, and concentrated behavior at 5% starch or above. After 24 h of storage at room temperature, syneresis was observed in some samples as the development of a transparent, aqueous layer over a turbid, gel-like layer, as in the case of 2% 75:25, in which the concentration of starch was below c^*. Similarly, Yoshimura, Takaya, and Nishinari (1999) studied the effects of xyloglucan on the gelatinization of corn starch, at different concentrations and polymer ratios. The degree of syneresis increased with decreasing corn starch concentration.

In other samples (20% 10:0), inulin precipitated after 24 h of storage. Additionally, limits of WMS dispersion in water were reached at concentrations of 40% 0:10. The three samples described above could not be analyzed and thus, the data points corresponding to these sample compositions are missing from the results and discussion.

3.2. Steady shear rheological analysis

The steady shear rheological characterization of the samples is shown in Fig. 1(a)–(f), at total polymer concentrations of 2, 5, 10 and 20%, respectively, at different inulin to WMS ratios. The data were well-behaved, presenting a low shear and high shear plateau in most cases. η decreased with increasing γ, corresponding to a shear-thinning behavior.

The experimental data were fitted to the Carreau model (Steffe, 1996):

$$\eta = \eta_\infty + (n_0 - n_\infty)[1 + (K\dot{\gamma})^2]^{(n-1)/2} \quad (1)$$

in which η = apparent viscosity, η_∞ = infinite-shear viscosity (at high $\dot{\gamma}$), η_0 = zero-shear viscosity (extrapolated to low values of $\dot{\gamma}$), K = consistency coefficient, and n = flow index. This model is represented by a line in Fig. 1; a good fit existed between the data and model. This model has been tested for use with other biopolymers such as high-methoxyl pectin, locust bean gum, and mixture of the two, and it was found to predict the η_0 values very close to experimental data (Chamberlain & Rao, 1999).

η decreased with increasing inulin content, indicating that inulin acted as a diluent to WMS. Thus, inulin did not interact synergistically with WMS to form a three-dimensional network. These results indicate that below 30%, inulin had not reached the c^* concentration. This behavior is contrary to that described by Utracki (1991) as an 'emulsion effect', in which the addition of the second phase causes an increase of the relative blend viscosity.

Data at total polymer concentrations of 30 and 40% are plotted in Fig. 1(e) and (f). At 30% 10:0 and 40%

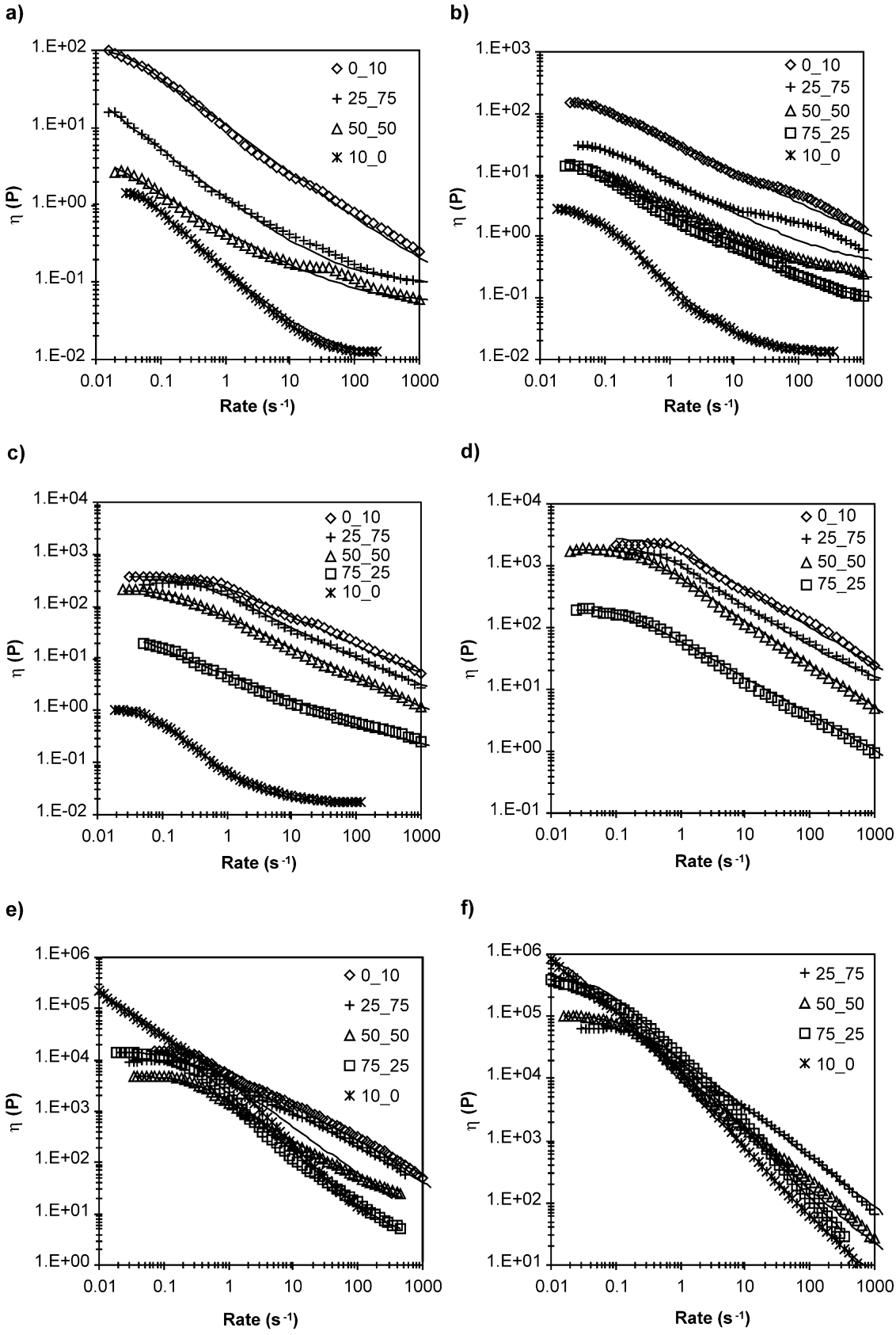

Fig. 1. Steady shear characterization of samples with a total polymer concentration of: (a) 2; (b) 5; (c) 10; (d) 20; (e) 30 and (f) 40% (w/w, w.b.), at different inulin to WMS ratios. Data fitted to the Carreau model (represented by a line).

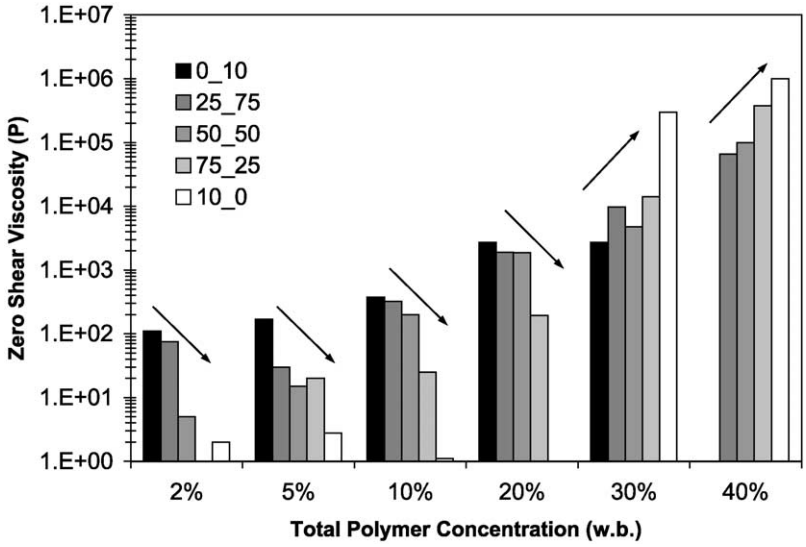

Fig. 2. Dependence of η_0 on total polymer concentration at different inulin to WMS ratios. Arrows represent trend in behavior. Missing data correspond to samples not analyzed due to phase separation before analysis.

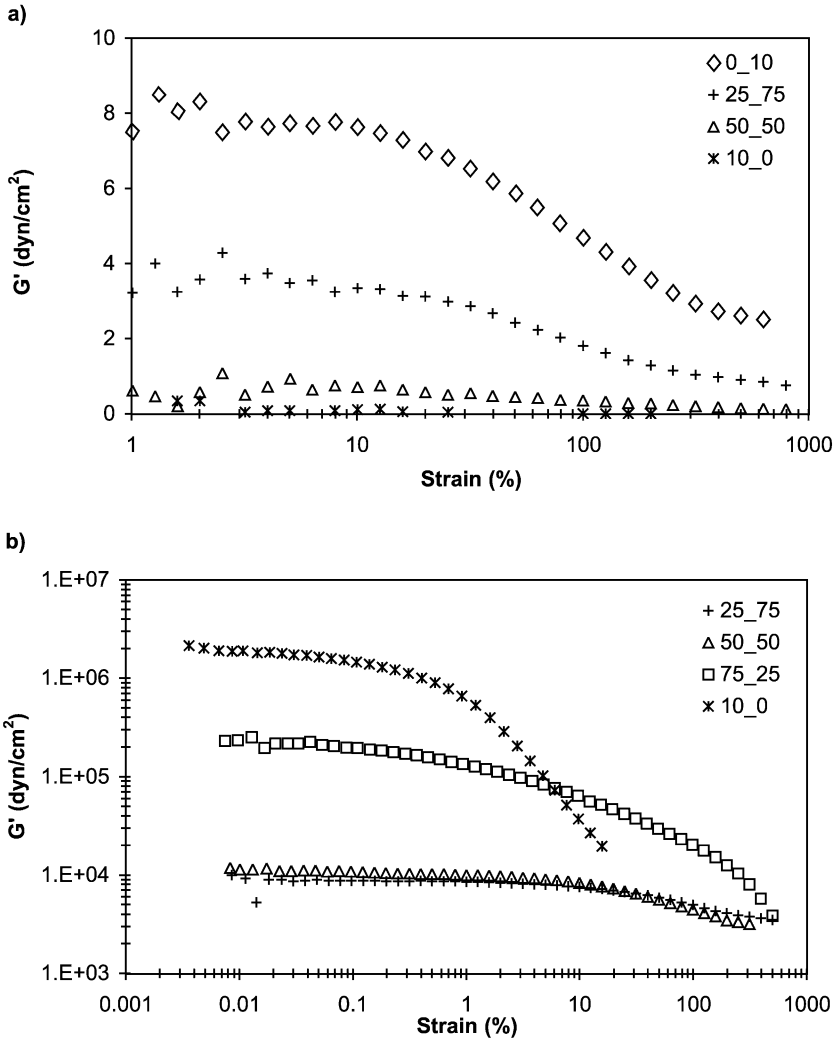

Fig. 3. Strain sweeps for (a) 2% and (b) 40% total polymer concentrations at different inulin to WMS ratios.

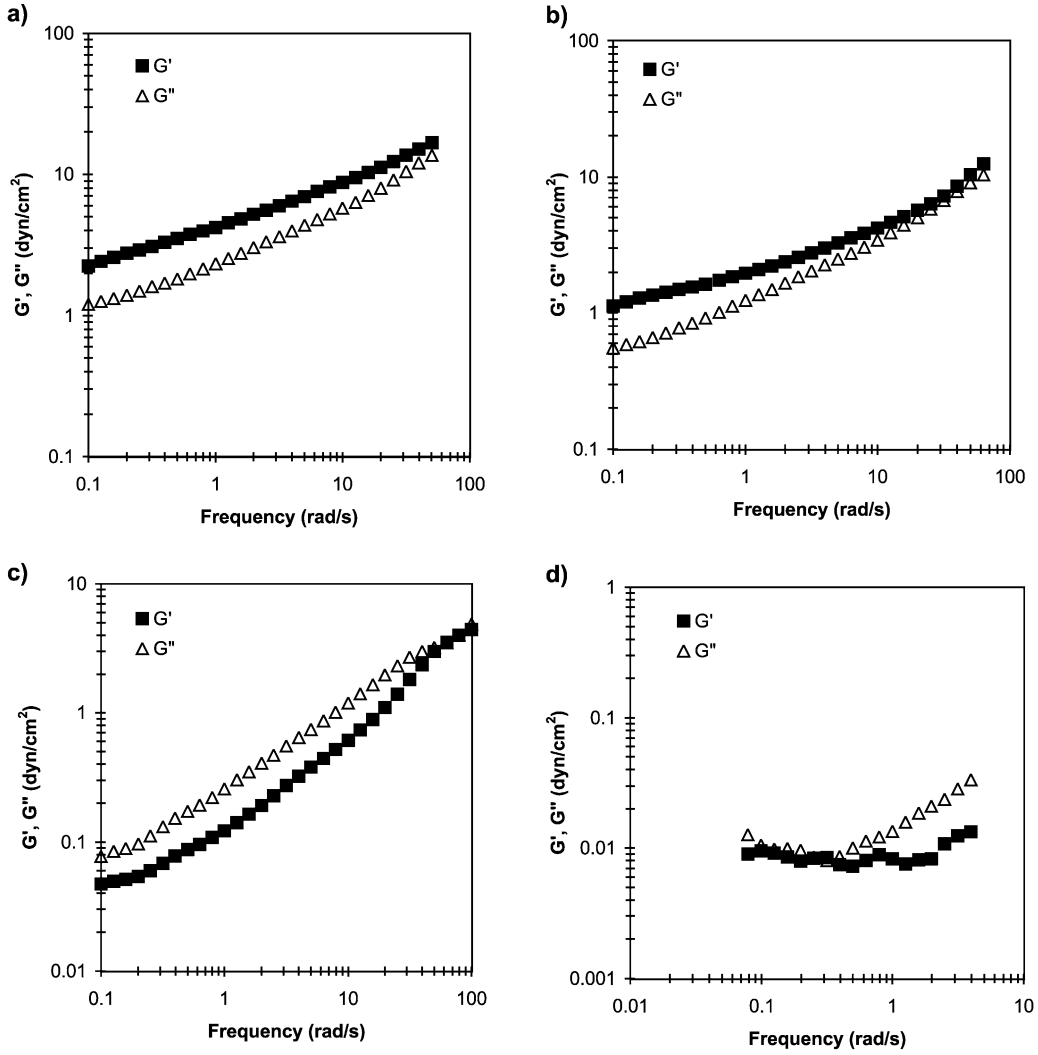

Fig. 4. Dynamic rheological data for samples with a total polymer concentration of 2% at inulin to WMS ratios of (a) 0:10, (b) 25:75, (c) 50:50 and (d) 10:0.

10:0 (pure inulin), a slope value close to -1 indicates the existence of yield stress behavior, which will be discussed later. A very important change in behavior was observed at 30% total polymer concentration: the monotonic decrease in η with increasing inulin content, observed at lower concentrations, was not present any more. In fact, at 40% concentration, the plateau viscosity (at low shear rates) increased with increasing inulin content. In order to illustrate this observation, the value of η_0 was calculated by fitting the data to the Carreau model (Eq. (1)). Fig. 2 represents a plot of η_0 vs. concentration, at different inulin to WMS ratios and the trend in behavior is represented by arrows. The following observations can be made: (a) η_0 increased with total polymer concentration; (b) up to 20% total polymer concentration, η_0 decreased with increasing inulin content, as indicated by the arrows; and (c) at total polymer concentrations $\geq$30% (w/w, w.b.), η_0 increased with increasing inulin content. A change in the rheological properties indicated that a phase inversion had occurred from a WMS-continuous system in which inulin formed the dispersed phase, to an inulin-continuous system in which WMS formed the dispersed phase. In the first scenario, WMS, the most elastic component, embedded inulin chains, which could not form a continuous network due to concentrations below inulin's c^* limit; in the second scenario, highly disintegrated starch granules became easily entrapped in the strong inulin network, favored by concentrations above inulin's c^*. These results confirm the findings by Utracki (1991), who stated that the concentration of phase inversion depends on the viscosity ratio and on the maximum packing volume fraction (c^*). Similar results were reported by Martinez and Williams (1980), who generated a plot of η vs. volume fraction (ϕ) of a component in a polymer blend, in which a monotonic increase in η with increasing ϕ was observed. Maxima in that plot were described as an interlocking of semi-continuous components (Martinez & Williams, 1980), at which a phase inversion was observed. Mohammed et al. (1998)

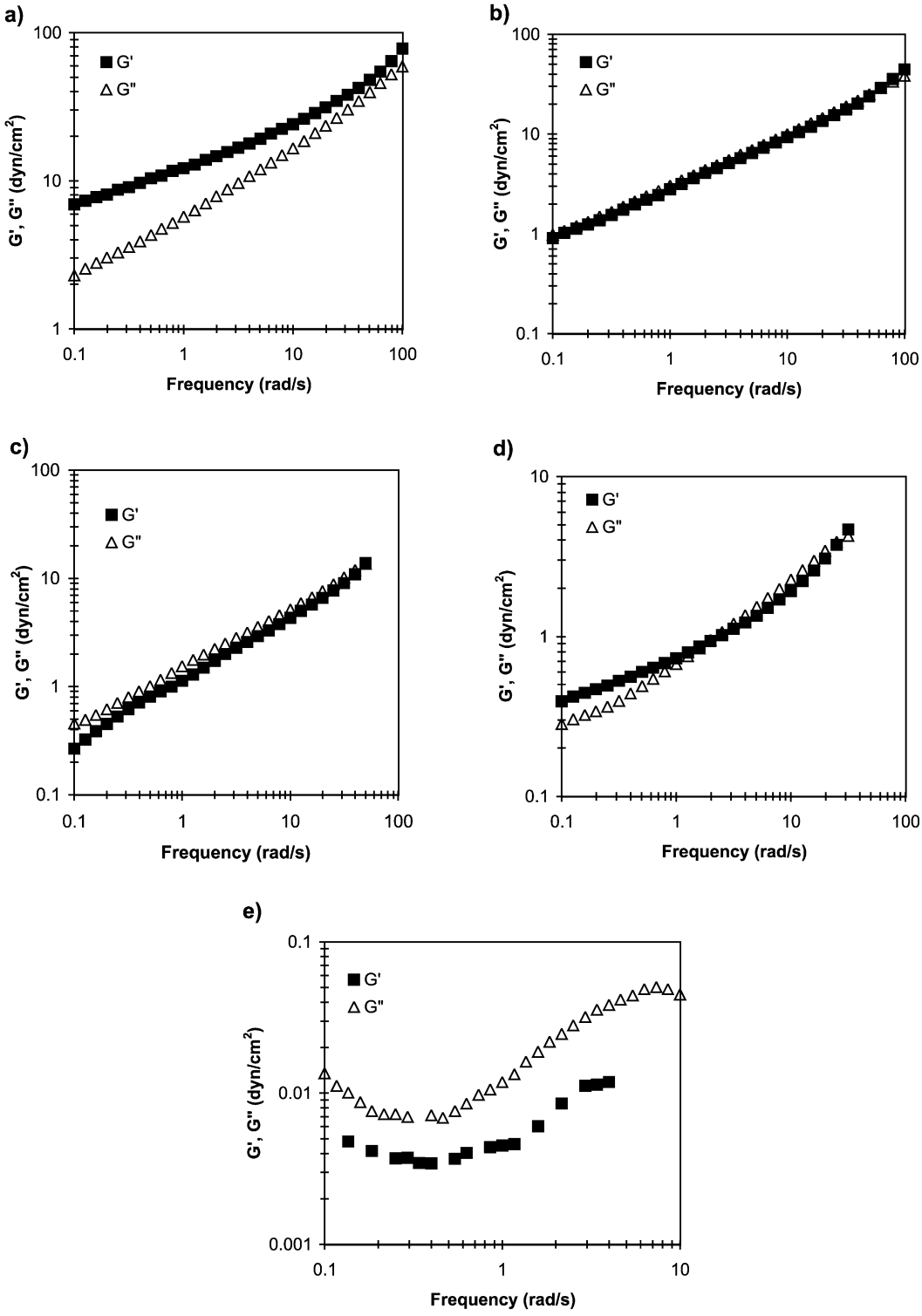

Fig. 5. Dynamic rheological data for samples with a total polymer concentration of 5% at inulin to WMS ratios of (a) 0:10, (b) 25:75, (c) 50:50, (d) 75:25 and (e) 10:0.

concluded that the distribution of two phases in WMS with other biopolymers (such as gelatin, xanthan and agarose) is determined by '(i) the ease of dissociation of the weak starch network formed on gelatinization, to reduce topological restrictions on formation of a stronger biopolymer matrix, and (ii) the extent to which the biopolymer promotes association of starch granules.' Other examples of investigators who used rheological

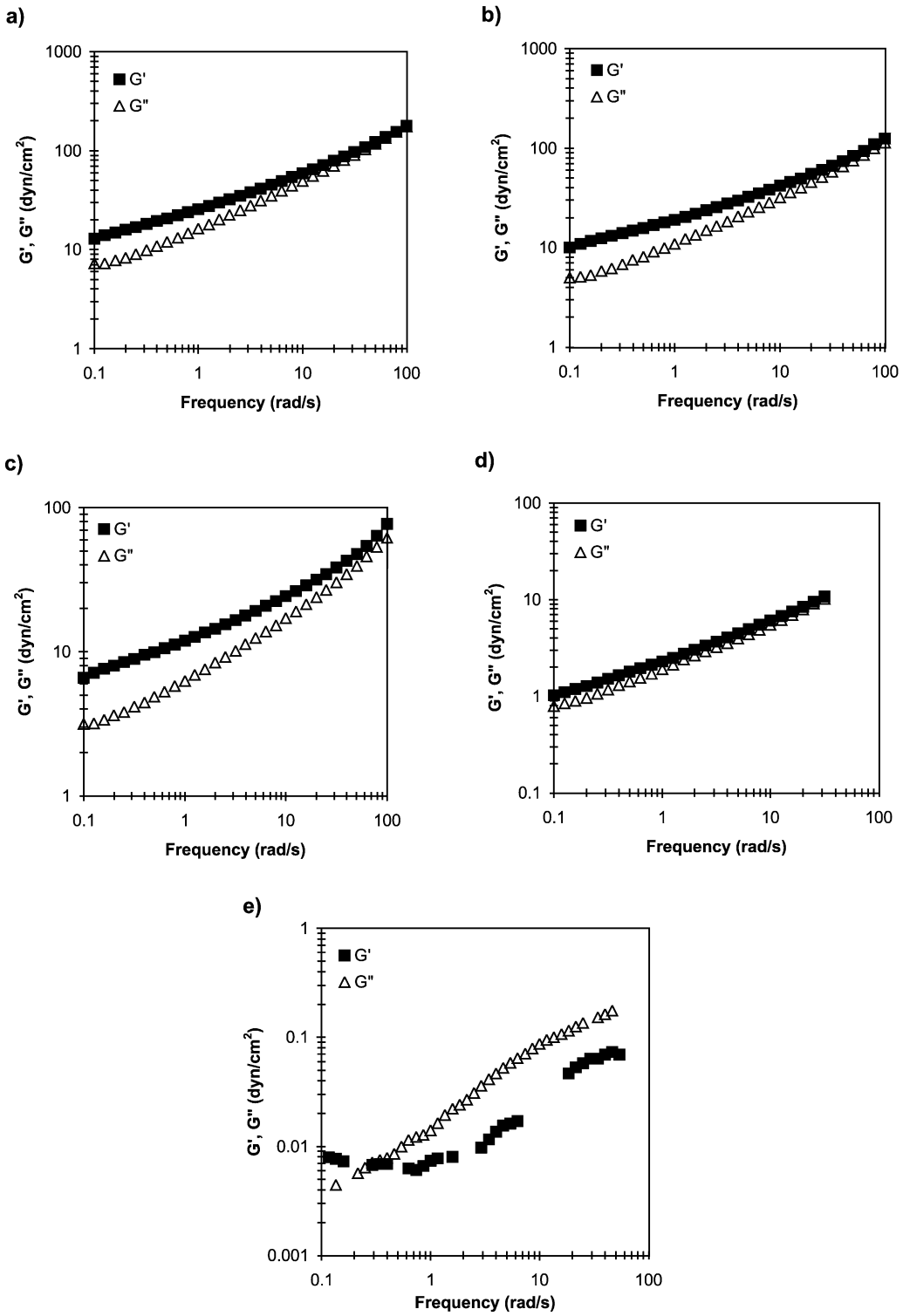

Fig. 6. Dynamic rheological data for samples with a total polymer concentration of 10% at inulin to WMS ratios of (a) 0:10, (b) 25:75, (c) 50:50, (d) 75:25 and (e) 10:0.

measurements to determine phase inversion phenomena include Kasapis, Morris, Norton and Brown (1993), who studied mixed gels of gelatin–maltodextrin systems, and Manoj et al. (1996) who investigated maltodextrin–caseinate systems.

3.3. Oscillatory rheological analysis

The property that defines a gel is its viscoelastic behavior. The limit of linear viscoelasticity, at which, in the present case, rheological properties are strain-independent, was

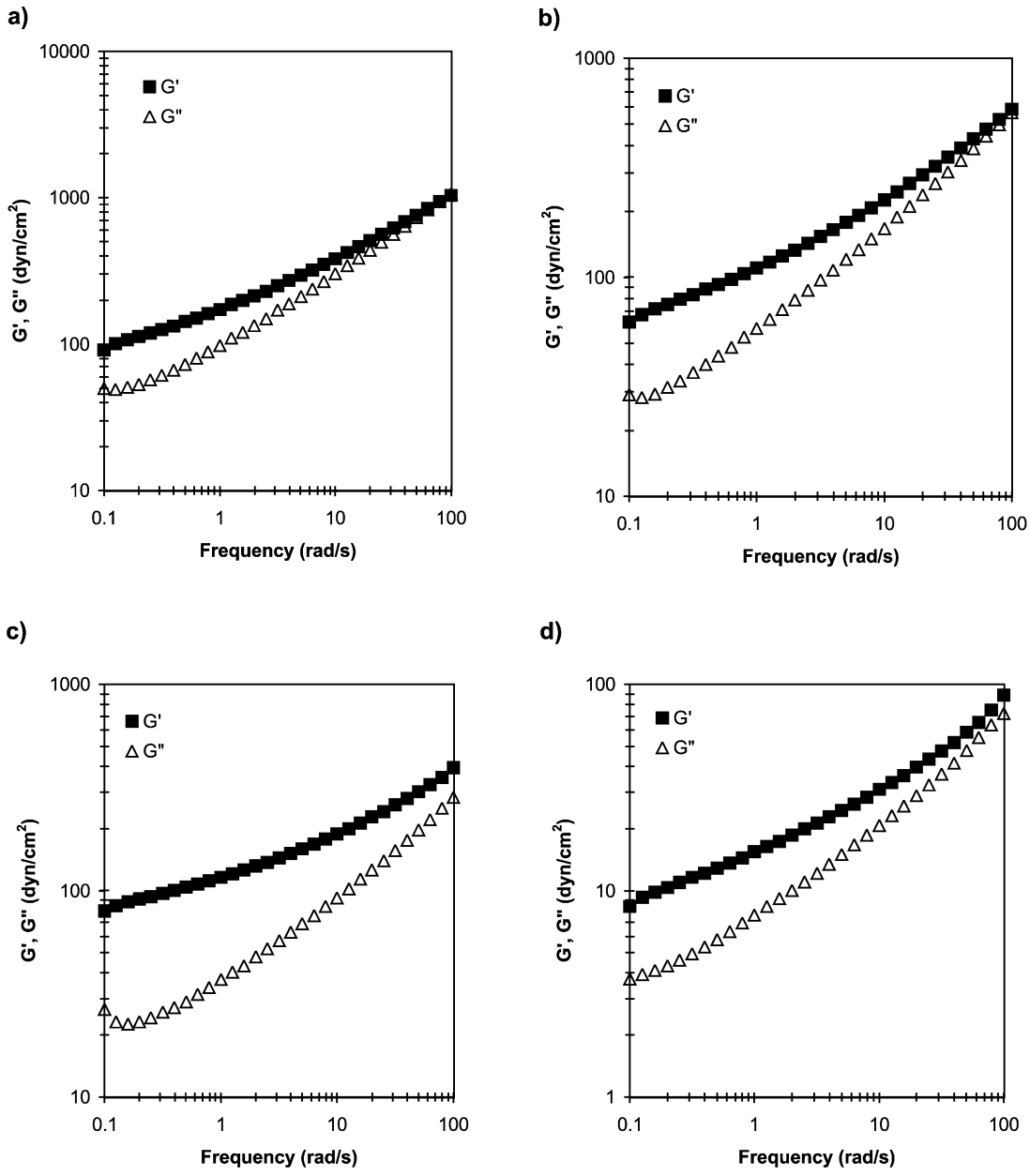

Fig. 7. Dynamic rheological data for samples with a total polymer concentration of 20% at inulin to WMS ratios of (a) 0:10, (b) 25:75, (c) 50:50 and (d) 75:25.

determined through strain sweep experiments. A critical strain value was identified on moduli vs. strain plots, corresponding to the maximum strain within the linear viscoelastic region. Fig. 3 shows typical strain sweeps plots for the two extreme concentrations: (a) 2% and (b) 40%, at different inulin to WMS ratios. Gels usually show a dependence of moduli on oscillatory strain in which G' remains independent up to the critical strain value, and then decreases when the sample starts to flow (Manoj et al., 1996). This behavior was followed by most of the samples represented in Fig. 3, except in the case of dilute systems, as in the case of 2% 10:0, which was little affected by strain. At 2% the magnitude of G' decreased with increasing inulin content, while at 40%, the opposite behavior was observed, confirming the previously discussed results observed through steady shear experiments. Thus, inulin disrupted the structure of WMS at low total polymer concentrations, while at high total polymer concentrations (above inulin's c^*), the rheological properties of the mixed system were dominated by those of inulin.

Fig. 4 shows results for 2% total polymer concentration at inulin to WMS ratios of (a) 0:10, (b) 25:75, (c) 50:50 and (d) 10:0. At no or low inulin concentrations (Fig. 4(a) and (b)), the samples presented typical characteristics of a weak gel system: the storage modulus was higher than the loss modulus ($G' > G''$) throughout the whole range of frequency, and both moduli were frequency-dependent. A change in behavior was observed at 2% 50:50 (Fig. 4(c)), in

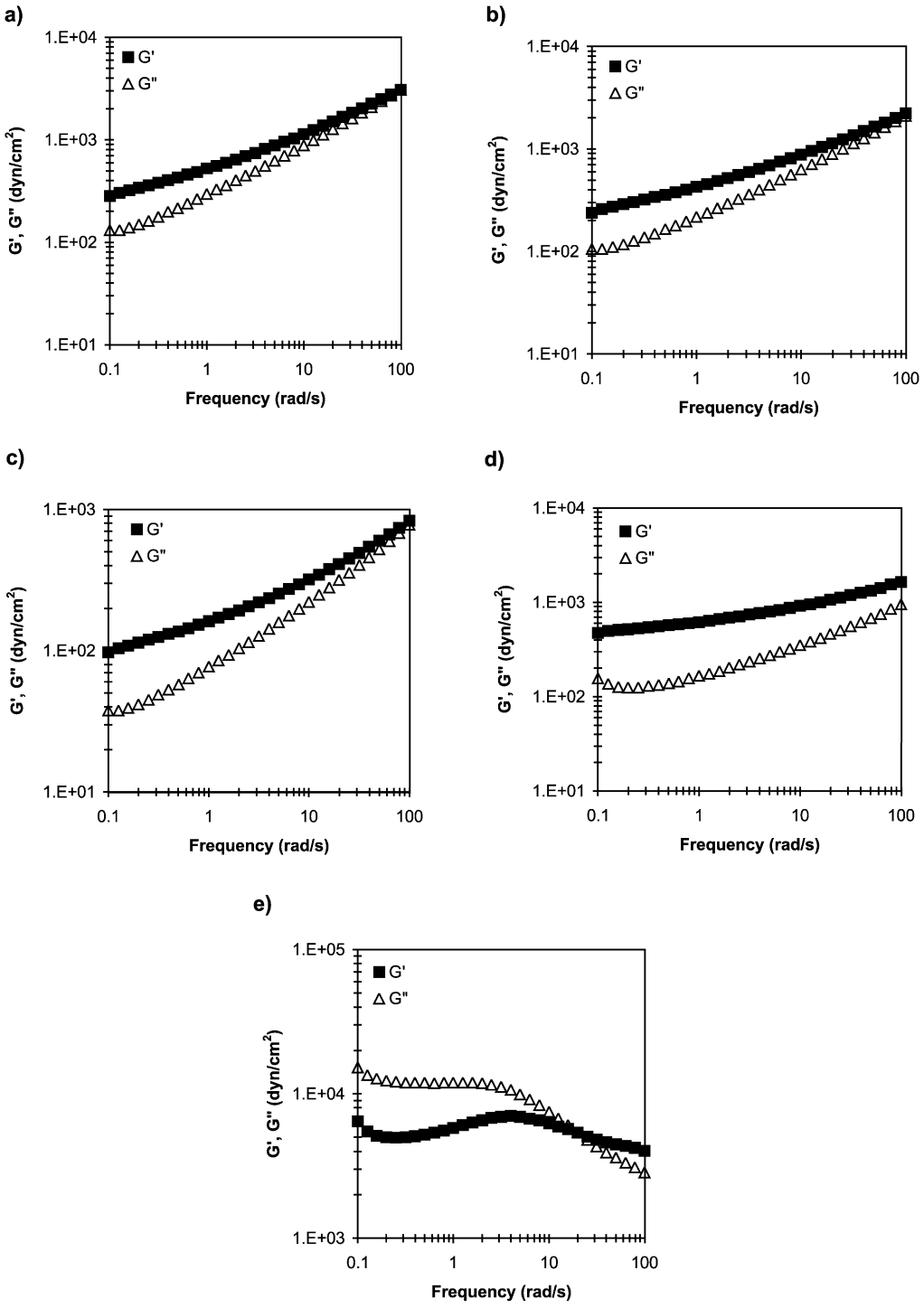

Fig. 8. Dynamic rheological data for samples with a total polymer concentration of 30% at inulin to WMS ratios of (a) 0:10, (b) 25:75, (c) 50:50, (d) 75:25 and (e) 10:0.

which characteristics of a non-gelling, liquid-like system were present: $G' < G''$ over the entire frequency range but approached each other at high frequencies, and a strong frequency dependence of both G' and G''. At this point, inulin interfered with the network formation properties of WMS, which can also be observed on the reduced order of magnitude of the moduli as compared to that of pure WMS Fig. 4(d), which corresponds to 2% 10:0 (pure inulin), also presented characteristics of a dilute solution. Thus, inulin's concentration was below c^*. Accordingly, pure inulin's moduli were two orders of magnitude smaller than that of pure WMS. Opposite behavior was observed by Closs, Conde-Petit, Roberts, Tolstoguzov, and Escher (1999), who determined that blends of starch and galactomannan showed

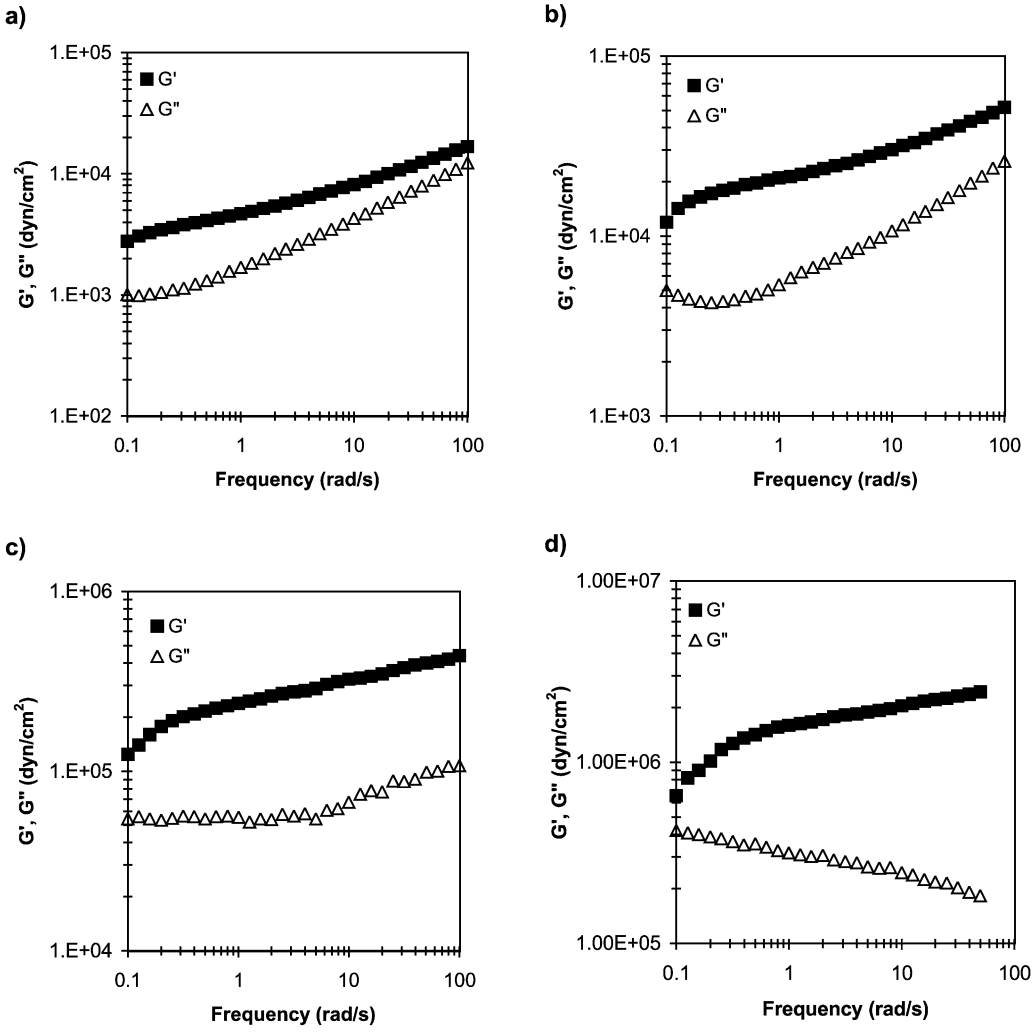

Fig. 9. Dynamic rheological data for samples with a total polymer concentration of 40% at inulin to WMS ratios of (a) 25:75, (b) 50:50, (c) 75:25 and (d) 10:0.

an increase in the structural strength of the blends, when compared to the individual components. In such case, the strengthening effect was caused by volume exclusion effects, rather than by synergistic interaction between starch and galactomannan.

In order to compare the effect of concentration on the rheological properties of the system, Figs. 5–9 represent samples at 5, 10, 20, 30 and 40% total polymer concentration, respectively. Following similar arguments than above, Fig. 5(a) (5% 0:10, pure WMS) showed characteristics of a weak gel. Fig. 5(b)–(d) (25:75, 50:50 and 75:25, respectively) showed more liquid-like behavior as G' became equal or greater than G'' and the moduli's magnitude decreased as inulin concentration increased. In Fig. 5(e) (10:0), inulin presented the behavior of a dilute solution, with very low moduli. At low frequency values, the observed 'dip' can be adjudicated to some time scale difference between measurement (longer time) and particles relaxation or reorganization (shorter time).

In the case of 10% total polymer concentration, most of the samples presented characteristics of weak gels (Fig. 6(a)–(d), 0:10 to 50:50). Fig. 6(e) (10:0, pure inulin) presents characteristics of a dilute system. Similar results were observed for 20% total polymer concentration (Fig. 7(a)–(d)), except for an increase in the magnitude of moduli due to increasing total polymer concentration. Results for pure inulin are unavailable due to the occurrence of syneresis before the samples were analyzed.

Fig. 8 represents samples at 30% total polymer concentration. Fig. 8(a)–(c) show characteristics of weak gels. A change in behavior is observed in Fig. 8(d) (75:25), in which the moduli's magnitude increased with the addition of inulin. A strong gel behavior was also observed: $G' > G''$ throughout the frequency range, and the moduli were nearly constant or frequency-independent. Results for pure inulin samples (10:0) are shown in Fig. 8(e), in which surprisingly, $G'' > G'$, indicating a 'liquid-like' behavior, although the moduli reached a high magnitude (10^4 dyn/cm^2). Then, the structure should correspond to one with no entanglements at

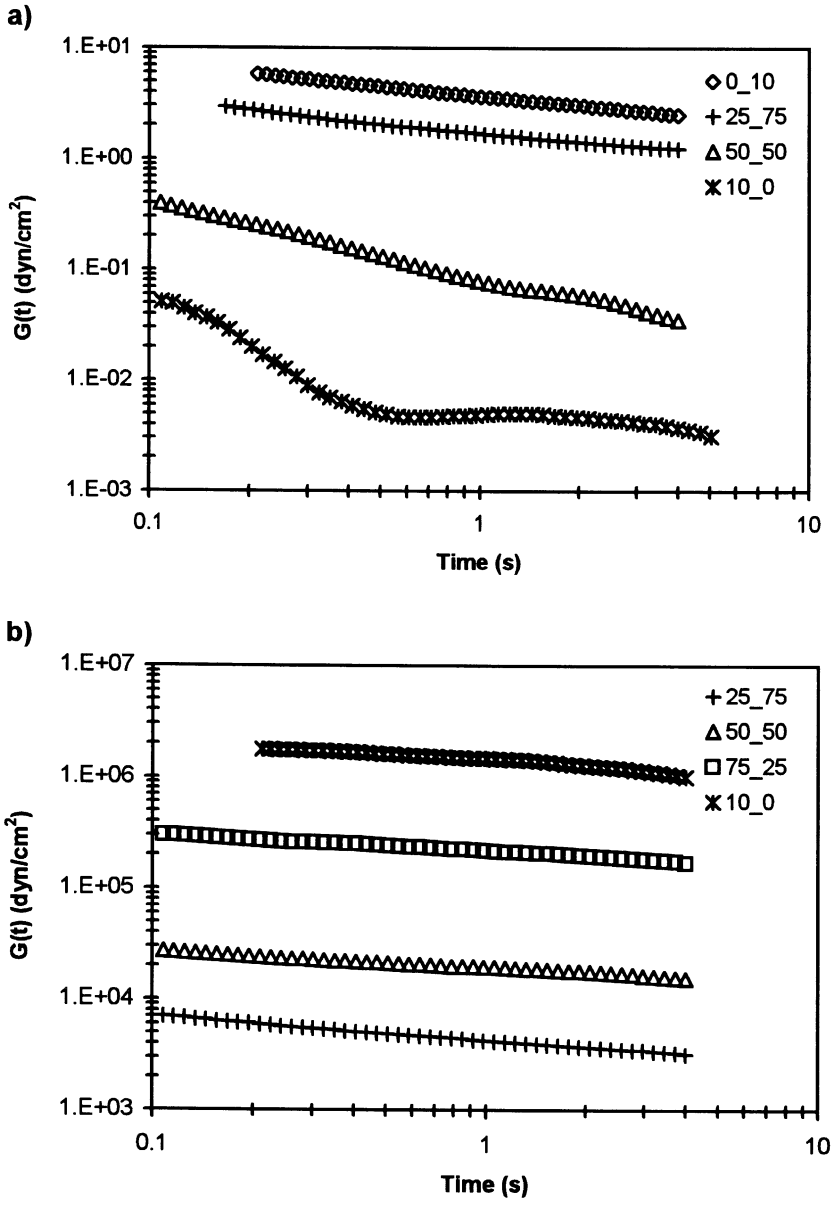

Fig. 10. Stress relaxation modulus for (a) 2% and (b) 40% total polymer concentrations at different inulin to WMS ratios.

all, with particles sliding one on top of the other, resulting in a 'liquid-like' behavior. At high frequencies there is a change in the material's response, indicating that the initial structure has been disrupted. Similar findings were obtained by Gray and Bonnecaze (1998), who studied the rheology of flowing dense suspensions. They explained this behavior as the bulk shearing of crystal grains rather than motion only at grain boundaries.

Results for samples at 40% concentration are presented in Fig. 9. Pure WMS was not examined because the dispersion limits of starch in water were exceeded. The moduli's magnitude increased with inulin content, thus indicating that the gels became stronger as more inulin was added. The difference between G' and G'' became larger and the moduli became more frequency-independent as inulin concentration increased, indicating more solid-like behavior. It is evident that at these concentrations, inulin exceeded c^* and that it was able to form a continuous, strong network. Pure inulin samples (40% 10:0) presented the typical characteristics of a highly crystalline polymer in which G' is relatively flat throughout the frequency range and G'' is considerably less than G''. The shape of both moduli follow those of a highly crystalline polymer, described by Ferry (1980). These results confirm the phase-inversion phenomena described before.

3.4. Stress relaxation analysis

The relaxation modulus, $G(t)$, was calculated from the dynamic data as indicated in Section 2. A plot of $G(t)$ vs. t is

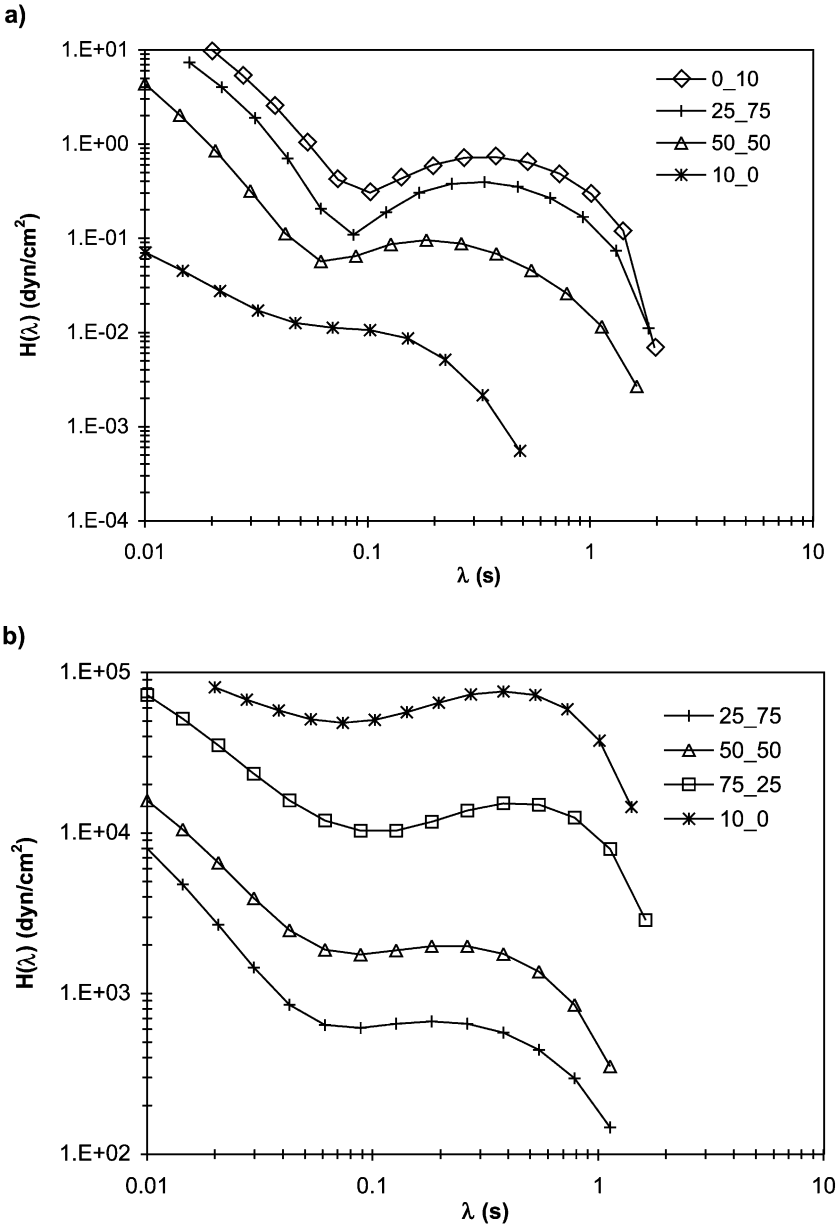

Fig. 11. Stress relaxation spectra for (a) 2% and (b) 40% total polymer concentrations at different inulin to WMS ratios.

shown in Fig. 10 for the two extreme total polymer concentrations of (a) 2% and (c) 40% at different inulin to WMS ratios. The effect on rheological properties was also captured by this type of plot, since the relaxation modulus decreased as inulin concentration increased at inulin concentrations below c^* (Fig. 10(a)), and the opposite behavior was observed above inulin's c^* (Fig. 10(b)). In Fig. 10(a), the sharper drop in 2% 10:0 (pure inulin) is an indication of a more liquid-like material, when compared to samples containing WMS, which show a very slow terminal relaxation zone. In Fig. 10(b), very little stress relaxation exists over time for these samples, indicating little backbone readjustments, characteristic of highly crystalline polymers (Ferry, 1980).

The relaxation spectrum, $H(\lambda)$, of each sample was also calculated from the dynamic data using the ARES Orchestrator software. The plot of $H(\lambda)$ vs. relaxation time (λ) is presented in Fig. 11 for the two sets of data plotted in Fig. 10. The spectra also followed the change in rheological behavior described above. In Fig. 10(a), the maximum shifts to shorter relaxation times with increasing inulin content, thereby indicating a structure containing fewer entanglements, since the gel structure is disrupted by inulin. In Fig. 10(b) the maximum sharpens and shifts to longer relaxation times with increasing inulin content, indicating a higher degree of structural organization (Ferry, 1980).

In order to demonstrate the consistency of the data, two samples were randomly chosen and subjected to stress

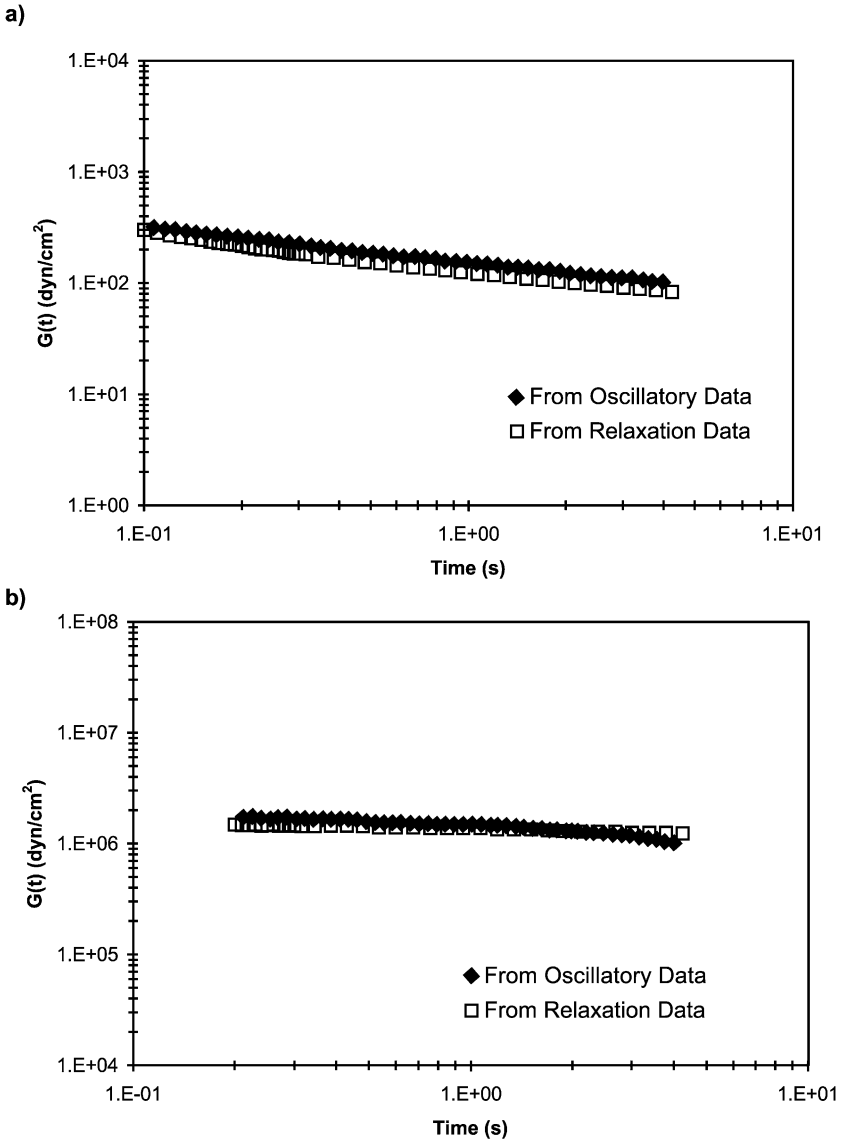

Fig. 12. Comparison between relaxation modulus derived from dynamic and relaxation data for (a) 20% 0:10 and (b) 40% 10:0.

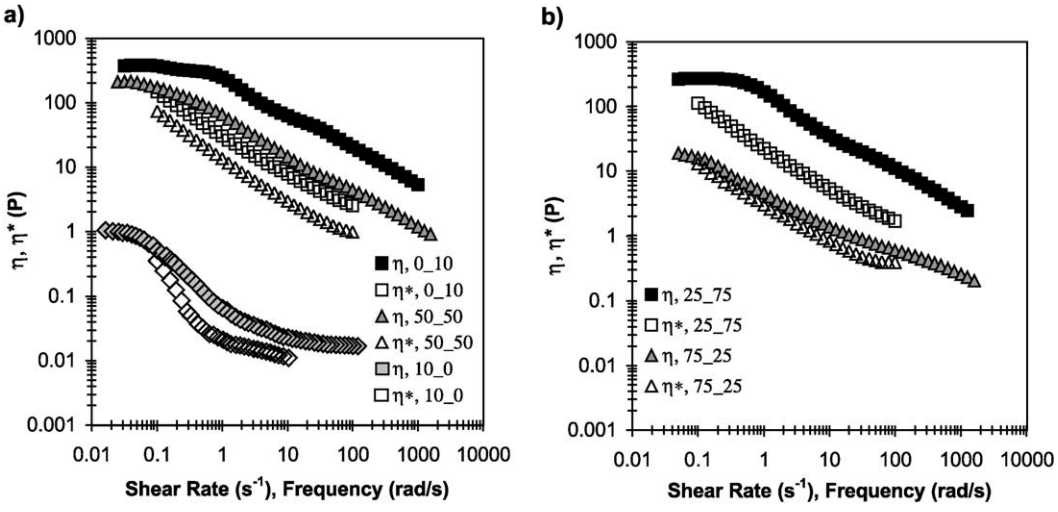

Fig. 13. Cox–Merz rule applied to samples with total polymer concentrations of 10% at inulin to WMS ratios of (a) 0:10, 50:50, 10:0; and (b) 25:75, 75:25.

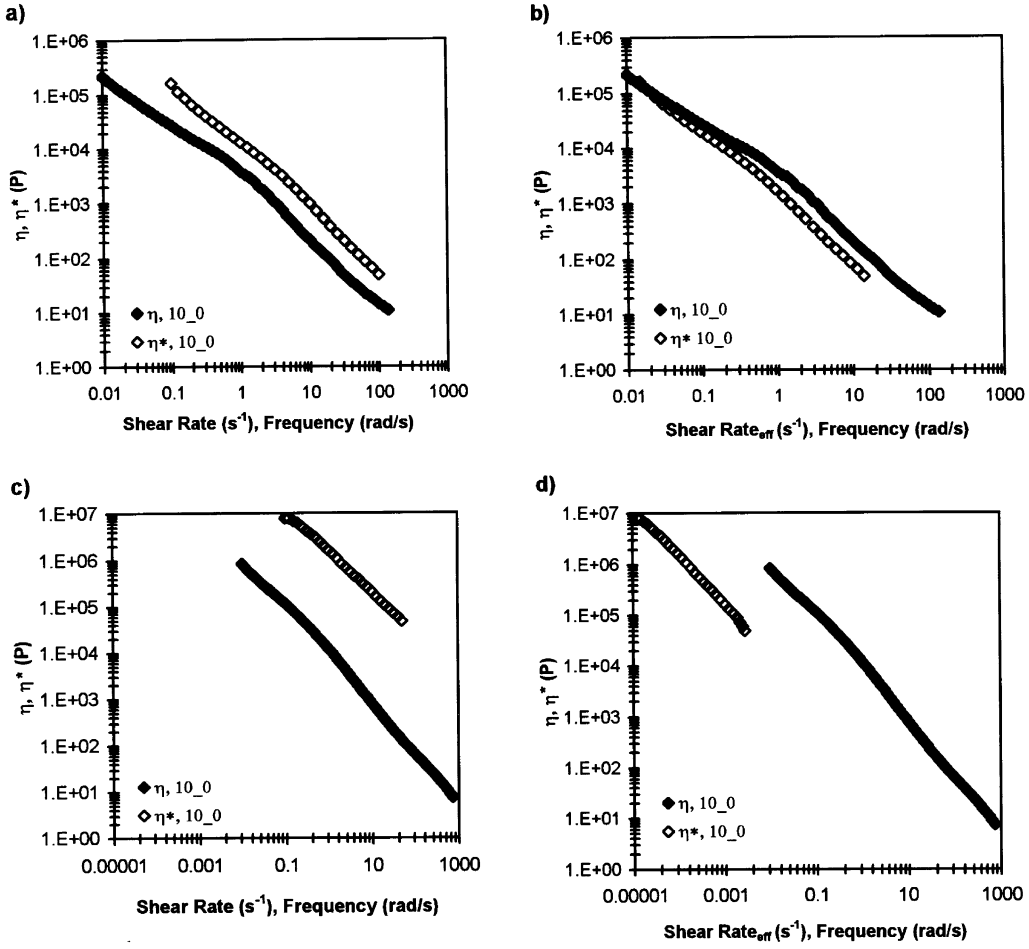

Fig. 14. 30% 10:0 (pure inulin) (a) before and (b) after extended Cox–Merz rule; 40% 10:0 (pure inulin) (c) before and (d) after extended Cox–Merz rule.

relaxation experiments as described in Section 2. A comparison between relaxation modulus derived from dynamic and relaxation data for (a) 20% 0:10 and (b) 40% 10:0 are plotted in Fig. 12, demonstrating a satisfactory agreement, thus indicating both reliable dynamic and relaxation data. A similar procedure was followed by Phan Thien and Safari-Ardi (1998) in analyzing rheological data for flour–water doughs.

3.5. Cox–Merz rule

The Cox and Merz, (1958) empirical rule relates complex viscosity (from oscillatory rheometry) to shear viscosity (from steady shear flow) as follows:

$$\eta(\dot{\gamma}) = |\eta^*(\omega)| \qquad \text{at } \dot{\gamma} = \omega \tag{2}$$

This rule has been found to be non-applicable to biopolymer dispersions with high-density entanglements or aggregates (Bistany & Kokini, 1983). Fig. 13(a) and (b) present results for a 10% sample at different inulin to WMS ratios, as an example of the general behavior followed by the samples. Note that the data was plotted in two figures to facilitate the interpretation of the graphs. Most samples did not follow the Cox–Merz rule, and showed greater divergence at high shear with $\eta > /\eta^*/$, similar to results found by Martinez and Williams (1980). As indicated by Soltero, Robles-Vásquez, and Puig (1995), η^* is usually larger than η, since structure is usually disturbed to a lesser extent by the small-amplitude dynamic tests than by steady shear tests. The trend followed by the experimental data ($\eta > /\eta^*/$) was also observed in (a) high-methoxy pectin dispersions, explained by a two-phase system of pectin micro-aggregates dispersed in the solvent; (b) aqueous solutions of hydroxyethyl guar gum, and (c) gelatinized 3–5% cross-linked WMS dispersions and 8% native WMS, due to the heterogeneous nature of the starch dispersions and to the highly branched structure of the WMS (Chamberlain & Rao, 1999). The Cox–Merz rule was only followed after WMS had been acid-converted for at least 45 min, during which enough amylopectin branches were cleaved to allow for the two viscosities to overlap (Chamberlain & Rao, 1999).

Doraiswamy et al. (1991), derived an extended Cox–Merz rule, which applies to concentrated suspensions and materials with yield stress. It consists of plotting η against $\dot{\gamma}$, and η^* vs. an effective shear rate, defined as $\gamma_m\omega$, where γ_m is the applied strain. The slope of the plot would be -1 at low effective shear rates (similar to yield stress behavior)

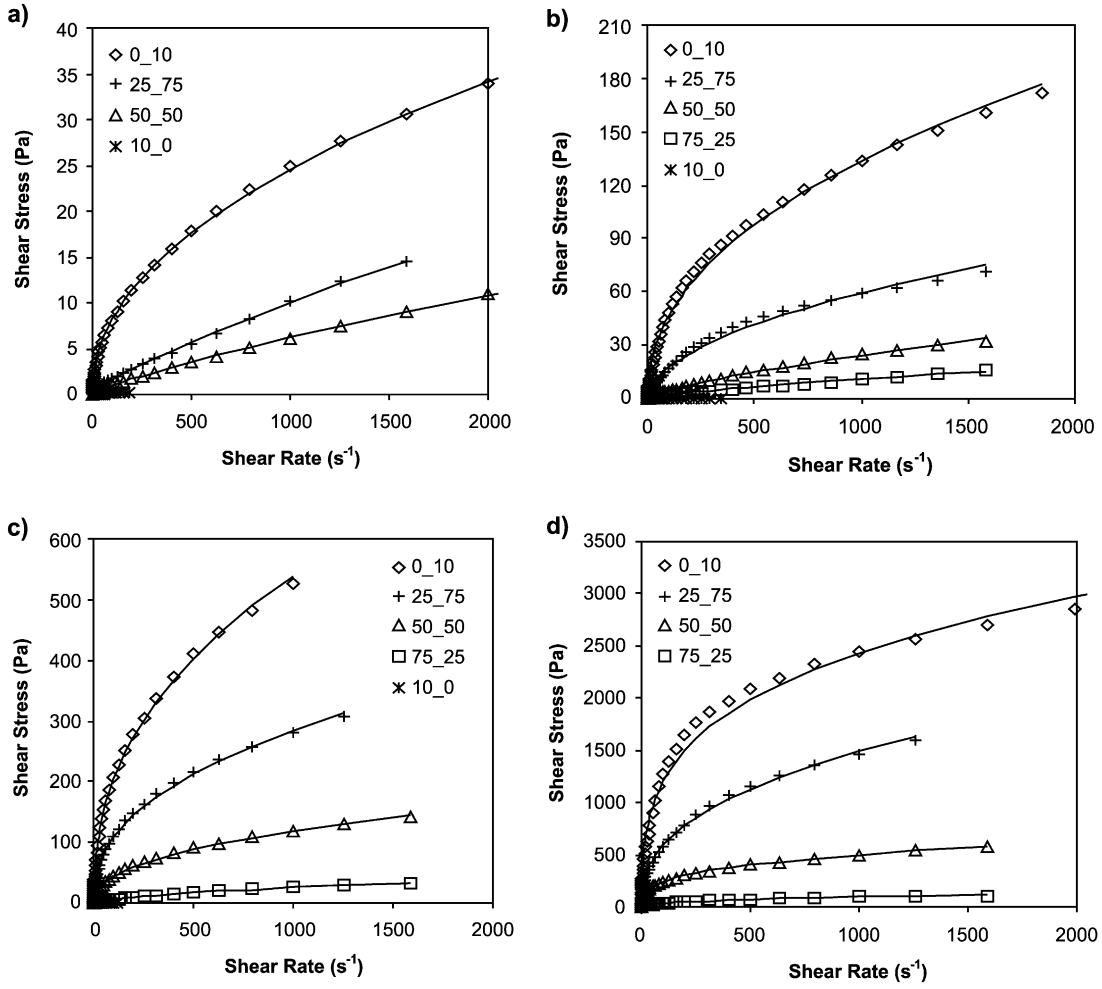

Fig. 15. Flow curves for samples with total polymer concentrations of (a) 2%, (b) 5%, (c) 10% and (d) 20% at different inulin to WMS ratios. Lines represent Herschel–Bulkley model calculations.

and to $n - 1$ at high effective shear rates (similar to power law behavior). According to Doraiswamy et al. (1991), this model is based on the assumptions of (a) elastic and viscous deformations occurring sequentially, not simultaneously, below and above the yield point, respectively, and (b) past the yield point, the recoverable or elastic strain remains constant at the level of the initial or 'critical' strain value at yielding, thus, the material is only capable of remembering the strain it undergoes as an elastic solid. Fig. 14(a) and (b) present results for 30% 10:0 (pure inulin) before and after the extended rule was applied. The extended Cox–Merz rule was followed by the 30% concentrated inulin suspension, thus making steady and dynamic shear results converge. Similarly, Fig. 14(c) and (d) show results for 40% 10:0, before and after the modification. In this case, the modified rule was not followed, although it switched the order of the data. In 1995, Soltero et al. reported that concentrated dispersions of surfactant-based lamellar liquid crystals did not follow the Cox–Merz rule due to orientation, breaking and aggregation of the liquid-crystalline microdomains due to high shear rates.

3.6. Herschel–Bulkley model and yield stress phenomena

Steady shear data for samples at high inulin concentrations indicated the existence of an apparent yield stress at low shear rates, as indicated by a slope of -1, and by the lack of a Newtonian plateau (Fig. 1). Fig. 15(a)–(d) show the flow curves for samples at 2, 5, 10 and 20% total polymer concentrations, respectively, fitted to the Herschel–Bulkley model (Steffe, 1996):

$$\sigma = K(\dot{\gamma})^n + \sigma_0 \tag{3}$$

in which σ = shear stress and σ_0 = yield stress, represented by a line in the figure. The values of the parameters that best fitted Eq. (3) are shown in Table 1. Below 20% total polymer concentration, an increase in inulin concentration induced Newtonian-like behavior, as observed from the lines becoming straighter as inulin concentration increases. Pure inulin samples below 20% showed typical Newtonian behavior ($n = 1$, $\sigma_0 = 0$). These results confirm those determined through dynamic oscillatory rheology, which

Table 1
Herschel–Bulkley model parameters for inulin–WMS samples at different total polymer concentrations and ratios

Total polymer concentration (w.b.) (%)	Inulin to WMS ratio	K (Pa s)	n	σ_0 (Pa)	R^2
2	0:10	0.90	0.48	0.02	1.00
	25:75	0.03	0.82	0.11	1.00
	50:50	0.02	0.81	0.04	1.00
	10:0	0.00	0.97	0.01	1.00
5	0:10	6.53	0.44	−3.28	1.00
	25:75	1.88	0.50	−1.47	1.00
	50:50	0.17	0.71	0.07	1.00
	75:25	0.06	0.76	0.22	1.00
	10:0	0.00	1.00	0.01	1.00
10	0:10	32.36	0.41	−11.08	1.00
	25:75	16.70	0.41	−3.49	1.00
	50:50	6.29	0.43	−0.87	1.00
	75:25	0.41	0.60	−0.08	1.00
	10:0	0.00	0.97	0.00	1.00
20	0:10	457.03	0.26	−311.70	1.00
	25:75	97.65	0.40	−13.21	1.00
	50:50	63.26	0.30	−9.55	1.00
	75:25	5.42	0.41	−0.28	1.00
30	0:10	1554.51	0.20	−961.07	1.00
	25:75	678.46	0.27	−286.47	1.00
	50:50	59.59	0.46	57.55	1.00
	75:25	0.39	0.91	130.98	1.00[a]
	10:0	0.00	4.93	142.22	0.83[a]
40	25:75	31,867.02	0.02	−29848.74	0.94
	50:50	4095.64	0.05	−2938.15	0.96
	75:25	−1.08	1.00	1309.90	0.96[a]
	10:0	−0.17	1.00	679.96	0.96[a]

[a] determined after extrapolating to zero shear rate.

indicated inulin's dilute solution behaviour, and inulin's action as a diluent.

When inulin was present at concentrations of 30% (Fig. 16(a) and (b)) and 40% (Fig. 16(c) and (d)), at ratios of 75:25 and 100:0, respectively, both dynamic and static yield stresses were observed. Static yield stress was identified as a maximum on the curve, caused by an unperturbed crystalline structure in inulin. Gray and Bonnecaze (1998) indicated that a high static yield stress of lattices indicates that when one crystallite can sustain the local stress, shear may occur in localized shear bands between crystal grains. In experiments by Husband et al. (1993), the static yield stress increased dramatically as the volume fraction of filler approached the volume fraction at maximum packing; with increasing volume percent solids, the exact static yield stress value became more difficult to determine.

A dynamic yield stress could also be calculated by extrapolation to low values of $\dot{\gamma}$. The values of the dynamic yield stress (σ_0) are presented in Table 1. It should be mentioned that negative values of yield stress lack any physical significance and thus, can be regarded as non-existing yield stress. Thus, concentrated inulin gels followed a Herschel–Bulkley rheological behavior ($0 < n < \infty$, $\sigma_0 > 0$). As indicated in the literature, there is no standard technique or instrument used to determine a material's yield stress quantitatively (Husband et al., 1993). The literature suggests that extrapolated yield stress depends on factors such as the rheological model, preservation of the material's structure, the accuracy of experimental data in the low shear rate region, and the time scale of the experiment (Zhu et al., 2001). In the present study, experiments were carried out under controlled conditions which allow for evaluation of yield stress (Zhu et al., 2001): low to high shear rates were used (thus, the structure was preserved at low shear rates), wall-slip effects were reduced using sandpaper on the plate surfaces, reliable steady shear viscosity data obtained for shear rates as low as 0.01 s^{-1}, and at least triplicate experiments resulted in very low variability.

4. Conclusions

The rheological response to shear flows, dynamic and relaxation measurements is strongly related to phase

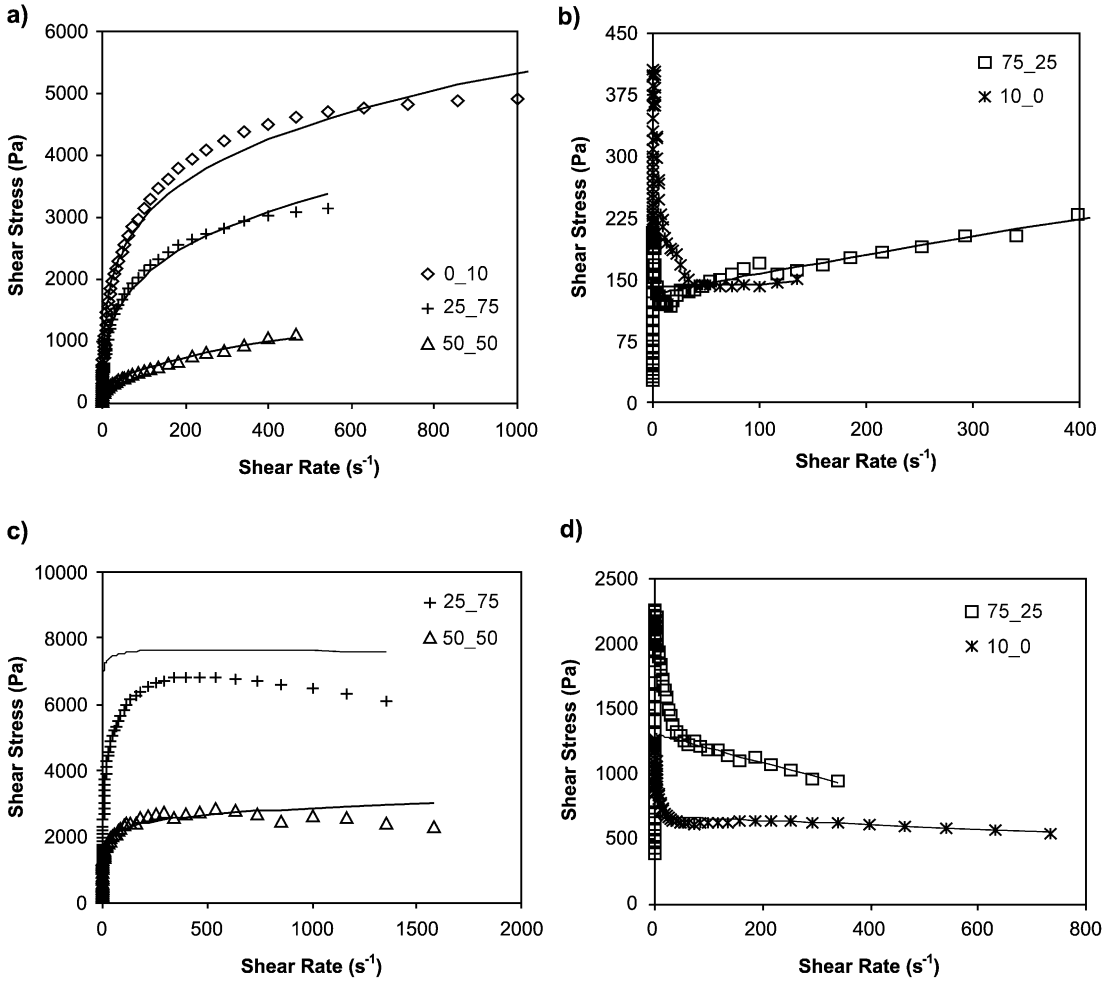

Fig. 16. Flow curves for samples with total polymer concentrations of 30% (a and b) and 40% (c and d) at different inulin to WMS ratios. Lines represent Herschel–Bulkley model calculations.

behavior and microstructure of the systems. In all the samples, η decreased with increasing $\dot{\gamma}$, corresponding to shear-thinning behavior. The suspected existence of yield stress from steady shear data was confirmed for concentrated inulin samples (30 and 40%) through fitting the data to the Herschel–Bulkley equation. A good fit existed between steady shear data and the Carreau model, which was used to estimate η_0. A change in the rheological properties (steady shear, dynamic and relaxation data) indicated that a phase inversion occurred when the samples changed from a WMS-continuous system with inulin as the dispersed phase (below inulin's c^*), to an inulin-continuous system with WMS as the dispersed phase (above inulin's c^*). Above c^*, inulin formed strong gels. The Cox–Merz rule was not followed by most of the inulin-WMS systems, since it has been found to be non-applicable to biopolymer dispersions with high-density entanglements or aggregates. The extended Cox–Merz rule was useful in analyzing concentrated inulin gels. The developed analytical methodology can be used as a model in the investigation of other carbohydrate–carbohydrate interactions via rheology. The resulting behavior between inulin and WMS can be used to interpret phenomena found in some food systems.

Acknowledgements

This is publication No. D-10544-4-02 of the New Jersey Agricultural Experiment Station supported by State Funds and the Center for Advanced Food Technology (CAFT). The Center for Advanced Food Technology is a New Jersey Commission on Science and Technology Center.

References

Abdulmola, N. A., Hember, M. W. N., Richardson, R. K., & Morris, E. R. (1996). Effect of xanthan on the small-deformation rheology of crosslinked and uncrosslinked waxy maize starch. *Carbohydrate Polymers*, *31*, 65–78.

Annable, P., Fitton, M. G., Harris, B., Phillips, G. O., & Williams, P. A. (1994). Phase behaviour and rheology of mixed polymer systems containing starch. *Food Hydrocolloids*, *8*(3/4), 351–359.

Astruc, M., & Navard, P. (2000). A flow-induced phase inversion in immiscible polymer blends containing a liquid-crystalline polymer studied by in situ optical microscopy. *Journal of Rheology*, *44*(4), 693–712.

Bistany, K. L., & Kokini, J. L. (1983). Comparison of steady shear rheological properties and small amplitude dynamic viscoelastic properties of fluid flood materials.. *Journal of Texture Studies*, *14*, 113–124.

Bonnecaze, R. T., & Brady, J. F. (1992). Yield stresses in electrorheological fluids. *Journal of Rheology*, *36*(1), 73–115.

Carriere, C. J. (1998). Evaluation of the entanglement molecular weights of maize starches from solution rheological measurements. *Cereal Chemistry*, *75*(3), 360–364.

Chamberlain, E. K., & Rao, M. A. (1999). Rheological properties of acid converted waxy maize starches in water and 90% DMSO/10% water. *Carbohydrate Polymers*, *40*, 251–260.

Closs, C. B., Conde-Petit, B., Roberts, I. D., Tolstoguzov, V. B., & Escher, F. (1999). Phase separation and rheology of aqueous starch/galactomannan systems. *Carbohydrate Polymers*, *39*, 67–77.

Cox, W. P., & Merz, E. H. (1958). Correlation of dynamic and steady flow viscosities. *Journal of Polymer Science*, *28*(118), 619–622.

Doraiswamy, D., Mujumdar, A. N., Tsao, I., Beris, A. N., Danforth, S. C., & Metzner, A. B. (1991). The Cox–Merz rule extended: A rheological model for concentrated suspensions and other materials with a yield stress. *Journal of Rheology*, *35*(4), 647–685.

Ferry, J. D. (1980). *Viscoelastic Properties of Polymers* (3rd). New York: Wiley, pp. 1–95, 321–403, 457–544.

Gray, J. J., & Bonnecaze, R. T. (1998). Rheology and dynamics of sheared arrays of colloidal particles. *Journal of Rheology*, *42*(5), 1121–1151.

Husband, D. M., Aksel, N., & Gleissle, W. (1993). The existence of static yield stresses in suspensions containing noncolloidal particles. *Journal of Rheology*, *37*(2), 215–235.

Kasapis, S., Morris, E. R., Norton, I. T., & Brown, R. T. (1993). Phase equilibria and gelation in gelatin/maltodextrin systems—Part III: Phase separation in mixed gels. *Carbohydrate Polymers*, *21*, 261–268.

Manoj, P., Kasapis, S., & Chronakis, I. S. (1996). Gelation and phase separation in maltodextrin–caseinate systems. *Food Hydrocolloids*, *10*, 407–420.

Martinez, C. B., & Williams, M. C. (1980). Viscosity and microstructure of polyethylene–poly(methyl methacrylate) melt blends: Some simple interpretations. *Journal of Rheology*, *24*(4), 421–450.

Mohammed, Z. H., Hember, M. W. N., Richardson, R. K., & Morris, E. R. (1998). Co-gelation of agarose and waxy maize starch. *Carbohydrate Polymers*, *36*, 37–48.

Niness, K. R. (1999). Inulin and oligofructose: What are they? *Journal of Nutrition*, *129*(7S), 1402S–1406S.

Phan Thien, N., & Safari-Ardi, M. (1998). Linear viscoelastic properties of flour–water doughs at different water concentrations. *Journal of Non-Newtonian Fluid Mechanics*, *74*, 137–150.

Roberfroid, M. B. (1999a). Caloric value of inulin and oligofructose. *Journal of Nutrition*, *129*, 1436S–1437S.

Roberfroid, M. B. (1999b). Concepts in functional foods: The case of inulin and oligofructose. *Journal of Nutrition*, *129*, 1398S–1401S.

Roberfroid, M. B. (2000). Prebiotics and probiotics: Are they functional foods? *American Journal of Clinical Nutrition*, *71*(6), 1682S–1687S.

Roberfroid, M., Gibson, G. R., & Delzenne, N. (1993). The biochemistry of oligofructose, a non-digestible fiber: An approach to calculate its caloric value. *Nutrition Review*, *51*(5), 137–146.

Schaller-Povolny, L. A., & Smith, D. E. (1999). Sensory attributes and storage life of reduced fat ice cream as related to inulin content. *Journal of Food Science*, *64*(3), 555–559.

Soltero, J. F. A., Robles-Vásquez, O., & Puig, J. E. (1995). Note: Thixotropic-antithixotropic behavior of surfactant-based lamellar liquid crystals under shear flows. *Journal of Rheology*, *39*(1), 235–240.

Steffe, J. F. (1996). *Rheological Methods in Food Process Engineering* (2nd). Michigan: Freeman Press, pp. 1–63.

Utracki, L. A. (1991). On the viscosity∇concentration dependence of immiscible polymer blends. *Journal of Rheology*, *35*(8), 1615–1637.

Yoshimura, M., Takaya, T., & Nishinari, K. (1999). Effects of xyloglucan on the gelatinization and retrogradation of corn starch as studied by rheology and differential scanning calorimetry. *Food Hydrocolloids*, *13*, 101–111.

Zhu, L., Sun, N., Papadopoulos, K., & De Kee, D. (2001). A slotted plate device for measuring static yield stress. *Journal of Rheology*, *45*(5), 1105–1122.

Zimeri, J. E., & Kokini, J. L. (2002). The effect of moisture content on the crystallinity and glass transition temperature of inulin. *Carbohydrate Polymers*, *48*, 299–304.

Zimeri, J. E., & Kokini, J. L. (2003). Phase transitions of inulin-waxy maize starch systems in limited moisture environments. *Carbohydrate Polymers*, *51*, 183–190 .